arXiv:astro-ph/0512461v1 17 Dec 2005

THE $M_{\mathrm{BH}} - \sigma_*$ RELATION IN LOCAL ACTIVE GALAXIES

Jenny E. Greene

Harvard-Smithsonian Center for Astrophysics, 60 Garden St., Cambridge, MA 02138

AND

Luis C. Ho

The Observatories of the Carnegie Institution of Washington, 813 Santa Barbara St., Pasadena, CA 91101

To appear in The Astrophysical Journal (Letters).

ABSTRACT

We examine whether active galaxies obey the same relation between black hole mass and stellar velocity dispersion as inactive systems, using the largest published sample of velocity dispersions for active nuclei to date. The combination of 56 original measurements with objects from the literature not only increases the sample from the 15 considered previously to 88 objects, but allows us to cover an unprecedented range in both stellar velocity dispersion ($30-268$ km s^{-1}) and black hole mass ($10^5 - 10^{8.6}$ $M_\odot$). In the $M_{\mathrm{BH}} - \sigma_*$ relation of active galaxies we find a lower zeropoint than the best-fit relation of Tremaine et al. (2002) for inactive galaxies, and an intrinsic scatter of 0.4 dex. There is also evidence for a flatter slope at low black hole masses. We discuss potential contributors to the observed offsets, including variations in the geometry of the broad-line region, evolution in the $M_{\mathrm{BH}} - \sigma_*$ relation, and differential growth between black holes and galaxy bulges.

Subject headings: galaxies: active — galaxies: kinematics and dynamics — galaxies: nuclei — galaxies: Seyfert

1. INTRODUCTION

Black holes (BHs) are a basic component of galaxies, and the existence of a tight correlation between the stellar velocity dispersion of bulges (σ_*) and the BH mass (the $M_{\mathrm{BH}} - \sigma_*$ relation; Gebhardt et al. 2000a; Ferrarese & Merritt 2000) suggests that the growth of the BH plays a fundamental role in the growth of the bulge, although exactly how remains unclear (e.g., Silk & Rees 1998; Kauffmann & Haehnelt 2000; Di Matteo et al. 2005). The $M_{\mathrm{BH}} - \sigma_*$ relation for inactive galaxies, in so far as it represents the final state of the BH-bulge system, represents a boundary condition for various evolutionary scenarios, and some clues are embedded in the scatter and possible skewness in the local $M_{\mathrm{BH}} - \sigma_*$ relation (Robertson et al. 2005). Unfortunately, the number of available points in the relation for inactive galaxies is limited, and statistics are poor. Currently, our only recourse is to rely on BH masses from active galactic nuclei (AGNs). To the extent that the BHs in AGNs continue to gain mass, the relation of BH masses in AGNs to their host bulges may carry additional information about the establishment of the relation for inactive sources. Since the majority of BH mass was assembled at high redshift (e.g., Yu & Tremaine 2002), we might expect to find the strongest evidence for evolution in the $M_{\mathrm{BH}} - \sigma_*$ relation at large cosmological distances (Shields et al. 2003; Treu et al. 2004; Walter et al. 2004; Peng et al. 2005). While undoubtedly this is a vital direction to pursue, there are a number of compelling reasons to study the local AGN $M_{\mathrm{BH}} - \sigma_*$ relation as well.

For one thing, while various methods are available to characterize the bulge potential, virial mass estimation (e.g., Ho 1999; Wandel et al. 1999; Kaspi et al. 2000), where the dense broad-line region (BLR) gas is assumed to be on Keplerian orbits around the central BH, is currently the most widely utilized tracer of BH mass. In the absence of a detailed model of the BLR, the zeropoint for the virial BH mass scale is set through a direct comparison with stellar velocity dispersions

for a small sample of local AGNs (Gebhardt et al. 2000b; Ferrarese et al. 2001; Nelson et al. 2004; Onken et al. 2004). The virial BH masses considered in these studies are remarkably consistent with the $M_{\mathrm{BH}} - \sigma_*$ relation of inactive galaxies, suggesting virial masses are reliable. But we must be cautious. For instance, there are compelling reasons to believe the BLR is actually a disk-wind (e.g., Murray & Chiang 1997; Proga et al. 2000; Proga & Kallman 2004) whose kinematics depend on both the mass and the accretion rate onto the BH. In this scenario, the virial mass calibration would depend systematically on BH mass and luminosity. We require objects spanning a wide range of AGN properties to properly calibrate the primary rung in our AGN BH "mass ladder." At the same time, we may hope to learn about evolution of the $M_{\mathrm{BH}} - \sigma_*$ relation by looking at the full distribution of local BHs (Robertson et al. 2005), and AGNs in particular (e.g., Yu & Lu 2004), in the $M_{\mathrm{BH}} - \sigma_*$ plane.

2. SAMPLE SELECTION AND METHODOLOGY

Our goal is to directly compare M_{BH} with σ_* for a large sample of AGNs. As outlined in Greene & Ho (2005c), we selected spectroscopically identified AGNs from the Third Data Release of the Sloan Digital Sky Survey (SDSS DR3; Abazajian et al. 2005) with $z \leq 0.05$ and signal-to-noise (S/N) ratios per pixel ≥ 18 in the region surrounding the Ca II $\lambda\lambda8498$, 8542, 8662 triplet (CaT). Here we consider the 32 objects from Greene & Ho (2005c) with resolved σ_* measurements and robust Hα line widths. To increase the sample, we have relaxed the z requirement and included an additional 24 galaxies to satisfy the criteria established by Greene & Ho for use of the "Fe region" (5250–5820 Å): S/N ≥ 20 ($\langle$ S/N $\rangle = 40 \pm 8$), estimated Eddington ratios [$L_{\mathrm{bol}}/L_{\mathrm{Edd}}$, where $L_{\mathrm{Edd}} \equiv 1.26 \times 10^{38}$ ($M_{\mathrm{BH}}/M_\odot$) ergs s^{-1}] $\lesssim 0.5$, and AGN contamination $< 80\%$. In addition to the 56 objects from the SDSS, we include 15 intermediate-mass BHs (IMBHs; $M_{\mathrm{BH}} \leq 10^6$ $M_\odot$) from Greene & Ho (2004) with σ_* measurements from Barth et al. (2005), resulting in a total

of 71 objects (see Table 1).

The stellar velocity dispersions are measured using a

Table 1. Sample Properties

Name (1)	z (2)	σ_* (3)	FWHM$_{H\alpha}$ (4)	log $L_{H\alpha}$ (5)	log M_{BH} (6)
SDSS J000805.62+145023.4	0.0454	140 ± 27	7610 ± 380	41.13 ± 0.04	7.7 ± 0.1
SDSS J004236.86−104921.8	0.0419	78.4 ± 10	1960 ± 97	41.58 ± 0.14	6.7 ± 0.1
SDSS J011703.58+000027.3	0.0456	98.8 ± 16	2270 ± 110	41.45 ± 0.08	6.8 ± 0.1

Note. — Col. (1): Name. Col. (2): Redshift. Col. (3): σ_* (km s^{-1}) measured from Ca triplet, unless otherwise noted. Col. (4): FWHM$_{H\alpha}$ (km s^{-1}). Col. (5): $L_{H\alpha}$ (ergs s^{-1}). Col. (6): $M_{BH} = (2.0 ^{+0.4}_{-0.3}) \times 10^6 \, M_\odot \, (L_{H\alpha}/10^{42}$ ergs s$^{-1})^{0.55\pm0.02}$ (FWHM$_{H\alpha}/10^3$ km s$^{-1})^{2.06\pm0.06}$ (Greene & Ho 2005b). Note that these are formal uncertainties; actual uncertainties in M_{BH} are probably dominated by systematics in BLR geometry. Table 1 is available in its entirety via the link to the machine-readable version above. A portion is shown here for guidance regarding its form and content.

direct pixel-fitting algorithm described in detail in Greene & Ho (2005c). The uncertainties are derived from simulations in which the AGN contamination and S/N ratio are varied for a grid of model galaxy spectra.

Virial masses are based on reverberation mapping (Blandford & McKee 1982), which uses the measured lag between variability in the photoionizing continuum and emission lines to estimate BLR radii. Currently there are 35 reverberation-mapped AGNs in the literature (Peterson et al. 2004). These, in turn, are used to calibrate the radius-luminosity relation, $R_{BLR} \propto L_{5100}^{0.64}$ (Greene & Ho 2005b; see also Kaspi et al. 2005), from which it is possible to infer a radius from the AGN luminosity. Combining the radius with an estimate of the velocity dispersion of the BLR yields a virial mass estimate for the BH, $M_{BH} = fR\,v^2/G$, where f is a factor that accounts for the geometry of the BLR. We assume $f = 0.75$ for a spherical BLR (Netzer 1990). Because our sample is selected to have strong stellar continua, virial BH mass estimation requires special care. Under these circumstances the most robust virial mass estimator is that based on the width and luminosity of the broad Hα emission line, as advocated by Greene & Ho (2005b). The emission-line fitting is described in Greene & Ho (2004, 2005b). Briefly, the stellar continuum is modeled and removed using a principal component analysis designed for the SDSS data by Lei Hao (Hao et al. 2005). We then construct a multi-component Gaussian model of the [S II] $\lambda\lambda6716$, 6731 doublet, which is shifted and scaled to fit the narrow Hα+[N II] $\lambda\lambda6548$, 6583 complex. The remaining (broad) Hα flux is fit with as many Gaussian components as needed to provide a statistically acceptable fit, although we attach no physical significance to the individual components. As described in Greene & Ho (2005b), we measure both FWHM$_{H\alpha}$ and the true second moment ($\sigma_{H\alpha}$) from the multi-component Gaussian fits. The uncertainties in the luminosities and line widths are derived using simulations, although we set a minimum uncertainty of $\sim 5\%$ on the line width.

3. RESULTS

We present the largest single collection of σ_* measurements in active galaxies. The single-epoch M_{BH} values for the SDSS and Barth et al. (2005) samples are estimated using FWHM$_{H\alpha}$ (rather than $\sigma_{H\alpha}$; e.g., Peterson et al. 2004). In our full sample, we also include the 15 reverberation-mapped AGNs considered by either Onken et al. (2004) or Nelson et al. (2004), using the weighted-mean σ_* from the two works. Weighted-mean virial products for this sample are computed using the Hβ lag and FWHM measurements presented in Peterson et al. (2004; the weights are calculated taking into account the asymmetric error bars), and BH masses

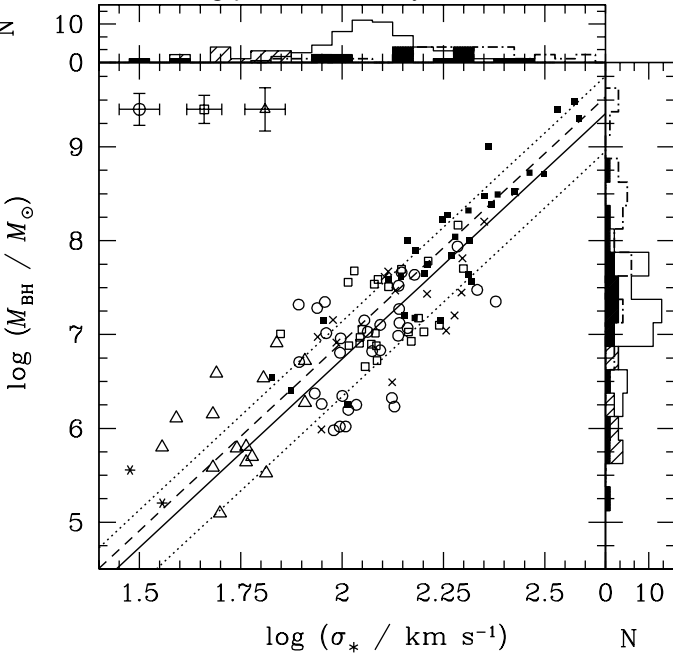are derived assuming $f = 0.75$. Finally, we include the well-

FIG. 1.— The $M_{BH}-\sigma_*$ relation for active and inactive galaxies. Open circles are measurements from this work using CaT, open squares are measurements using the 5250–5820 Å Fe region (see Greene & Ho 2005c), and open triangles represent the Keck data from Barth et al. (2005) but with M_{BH} recalculated using FWHM$_{H\alpha}$ values from DR3. Literature data include those of Onken et al. (2004) and Nelson et al. (2004; crosses; BH masses from Peterson et al. 2004), NGC 4395 and POX 52 (Filippenko & Ho 2003; Peterson et al. 2005; Barth et al. 2004; asterisks), and the primary sample of inactive galaxies with dynamically determined values of M_{BH} (Tremaine et al. 2002; filled squares). Representative error bars are shown in the upper left for the SDSS and Keck measurements. The dashed line represents the fit for the $M_{BH}-\sigma_*$ relation of inactive galaxies as given by Tremaine et al. (2002). The solid line is our best fit for the AGN sample with a fixed slope of $\beta = 4.02$ and $\alpha = 7.96 \pm 0.03$; the dotted lines show the measured intrinsic scatter of 0.4 dex. We display histograms of the σ_* (top) and M_{BH} (right) distributions for the Keck (shaded), SDSS (open), literature (filled), and inactive (dash-dot line) samples.

studied intermediate-mass BHs in NGC 4395 (reverberation mass $M_{BH} = 3.6 \times 10^5 \, M_\odot$, Peterson et al. 2005; virial mass $M_{BH} = 1.4 \times 10^4 \, M_\odot$, Filippenko & Ho 2003) and in POX 52 (virial mass $M_{BH} = 1.6 \times 10^5 \, M_\odot$, Barth et al. 2004). The full sample of 88 objects covers a range in mass of $10^5 - 10^{8.5} \, M_\odot$, and a corresponding range in σ_* of $30 - 268$ km s^{-1} (see Table 1). Consistent with previous work, Figure 1 shows that active galaxies apparently follow the $M_{BH} - \sigma_*$ relation defined by inactive systems, even with a sample size increased by a factor of nearly 6. In detail, however, we do find significant differences in zeropoint and slope compared to the inactive sample, which we describe below.

Assuming a log-linear form for the $M_{BH} - \sigma_*$ relation, $\log(M_{BH}/M_\odot) = \alpha + \beta\log(\sigma_*/\sigma_0)$, with $\sigma_0 = 200$ km s^{-1}, we can formally quantify deviations of AGNs from the $M_{BH} - \sigma_*$ relation of inactive systems. We use the Levenberg-Marquardt algorithm as implemented by *mpfit* to minimize χ^2, defined, following Tremaine et al. (2002), as

$$\chi^2 \equiv \sum_{i=1}^{N} \frac{(y_i - \alpha - \beta x_i)^2}{\epsilon_{yi}^2 + \beta^2 \epsilon_{xi}^2}, \tag{1}$$

where x_i correspond to $\sigma_{*,i}$, y_i to $M_{BH,i}$, and ϵ_i to the formal uncertainties in each measurement. In order to account for asymmetric uncertainties in each parameter, at each iteration ϵ_i is

selected to reflect the sign of $y_i - \alpha - \beta x_i$. In the simplified case of symmetric errors, we recover the results of the Numerical Recipes routine *fitexy* (Press et al. 1992) as implemented in IDL. We begin by fixing the slope β to the best-fit value of 4.02 from Tremaine et al. and investigate potential offsets in zeropoint. We find, for our sample alone, a best-fit $\alpha = 7.96 \pm 0.03$, which corresponds to an offset of -0.17 ± 0.07 from the value of $\alpha = 8.13 \pm 0.06$ of Tremaine et al. (consistent with Gebhardt et al. 2000b; Nelson et al. 2004; Onken et al. 2004; see summary in Table 2). The offset increases to -0.21 ± 0.06 when the literature values are included (using either the reverberation-mapped or virial mass for NGC 4395). Note that we are using formal uncertainties in $M_{\rm BH}$, while the true uncertainties are probably dominated by our ignorance of the BLR geometry and the corresponding uncertainty in how to extract the velocity dispersion of the virialized BLR from the observed line profile. Following Tremaine et al. and Gebhardt et al. (2000a), we estimate the intrinsic scatter as the value ϵ_0 that, when added to ϵ_y, results in a minimum χ_r^2 of 1. For both our sample alone and including the literature sample, we find an intrinsic scatter[1] of $\epsilon_0 = 0.4$ (dotted lines in Fig. 1). This is to be compared with the estimated scatter of 0.25-0.3 dex for the inactive sample (Tremaine et al. 2002). While there is probably intrinsic scatter in the underlying $M_{\rm BH}-\sigma_*$ relation, we conservatively adopt 0.4 dex as the systematic uncertainty in the single-epoch $M_{\rm BH}$ measurements, so that we bracket the full range in possible uncertainty. If we repeat the fitting above increasing the uncertainties in the single-epoch BH masses by 0.4 dex in quadrature, the results for our sample alone are virtually unchanged, while we find $\alpha = 7.86 \pm 0.04$ for the full sample, which corresponds to an offset of -0.27 ± 0.07. This offset is similar to that advocated by Onken et al., but it is statistically much more robust, being based on a final sample that is nearly 6 times larger.

When we fit both the zeropoint and slope, we obtain $\alpha = 7.84 \pm 0.04$ and $\beta = 3.65 \pm 0.13$ ($\alpha = 7.89 \pm 0.05$, $\beta = 3.74 \pm 0.17$) if we include (exclude) literature values, corresponding to slopes flatter than the value of $\beta = 4.02 \pm 0.32$ for inactive sources by -0.37 ± 0.35 (-0.28 ± 0.36). Including the 0.4 dex scatter to the single-epoch measurements yields an even flatter slope, with $\alpha = 7.79 \pm 0.04$ and $\beta = 3.49 \pm 0.18$ ($\alpha = 7.68 \pm 0.10$, $\beta = 2.95 \pm 0.32$). It appears that much of the flattening is driven by objects with BH masses $< 10^6 M_\odot$, which rely on an extrapolation of the radius-luminosity relation and thus may be suspect. [As pointed out by Barth et al. (2005), these objects also may be biased by selection toward large $M_{\rm BH}$ at a given σ_*.] When we remove the Barth et al. objects, as well as POX 52 and NGC 4395, but include all other data, we find $\beta = 4.19 \pm 0.22$ with the formal errors, or $\beta = 3.85 \pm 0.25$ with the additional 0.4 dex uncertainty added. The fact that the slope is still shallower when the (more realistic) uncertainties are included gives us some confidence that the flattening is real.

4. IMPLICATIONS AND CONCLUSIONS

We have established, with statistical confidence for the first time, that the $M_{\rm BH}-\sigma_*$ relation of local AGNs, while generally similar to that of inactive galaxies, shows some significant differences. We find evidence for a lower zeropoint, shallower slope, and (probably) larger scatter. There are many competing effects, relating both to BLR physics and galaxy evolution,

Table 2. Fit Parameters

Sample (1)	Uncertainties (2)	α (3)	β (4)
Our	Formal	7.96 ± 0.03	4.02
Full	Formal	7.92 ± 0.02	4.02
Our	Systematic	7.97 ± 0.06	4.02
Full	Systematic	7.86 ± 0.04	4.02
Our	Formal	7.89 ± 0.05	3.74 ± 0.17
Full	Formal	7.84 ± 0.04	3.65 ± 0.13
Our w/o IMBH	Formal	8.02 ± 0.08	4.61 ± 0.37
Full w/o IMBH	Formal	7.89 ± 0.04	4.19 ± 0.22
Our	Systematic	7.68 ± 0.10	2.95 ± 0.32
Full	Systematic	7.79 ± 0.04	3.49 ± 0.18
Our w/o IMBH	Systematic	7.66 ± 0.13	2.88 ± 0.54
Full w/o IMBH	Systematic	7.81 ± 0.05	3.85 ± 0.25

Note. — Col. (1): Data set considered; the sample "w/o IMBH" excludes the Barth et al. (2005) objects, POX 52, and NGC 4395. Col. (2): Adopted uncertainties. Col. (3): Zeropoint assuming $\log(M_{\rm BH}/M_\odot) = \alpha + \beta \log(\sigma_*/200 \text{ km s}^{-1})$. Col. (4): $M_{\rm BH}-\sigma_*$ slope, fixed to 4.02 for the first 4 entries.

that may contribute to the observed differences. If we posit that AGNs obey the relation of inactive galaxies exactly, then the scatter and zeropoint offset may be attributed to variations in the geometry of the BLR. This is the assumption made by Onken et al. (2004), who derive a statistical offset in the factor f that scales all BH masses upwards relative to the case of a spherical BLR. If, however, as suggested by disk-wind models (e.g., Proga & Kallman 2004), the geometry of the BLR depends on physical properties of the AGN such as the BH mass and the Eddington ratio, then virial mass estimates will not scatter randomly about one fixed value of f. Rather, f will change systematically with the state of the system, and its average value for any given sample will depend on the range of parameter space spanned by the objects used to derive it. It is important to recognize that all work so far—including ours—has considered a rather limited range in $M_{\rm BH}$ and $L_{\rm bol}/L_{\rm Edd}$, and so may lead to a biased value of f. Apart from the Greene & Ho (2004) objects studied by Barth et al. (2005), the practical challenge of detecting stellar absorption features to measure σ_* inevitably biases the final sample toward relatively low Eddington ratios and BH masses. Excluding the Barth et al. objects, the sample summarized in Figure 1 has a median $L_{\rm bol}/L_{\rm Edd} = 6 \times 10^{-2}$ and $10^6 \lesssim M_{\rm BH} \lesssim 10^8 M_\odot$. While we expect that secondary parameters (e.g., $L_{\rm bol}/L_{\rm Edd}$) may ultimately help to account for the overall scatter in the AGN $M_{\rm BH}-\sigma_*$ relation, we refrain from discussing this issue here because we believe that a proper analysis would require a larger and more complete sample than is currently available.

Apart from systematic uncertainties in virial masses, evolution of the $M_{\rm BH}-\sigma_*$ relation with cosmic time (e.g., Shields et al. 2003; Treu et al. 2004; Walter et al. 2004; Peng et al. 2005) also imprints scatter and skewness into the local relation as a function of $M_{\rm BH}$ (Robertson et al. 2005). However, it is unclear at this stage how much scatter can be attributed to the fact that BHs in AGNs, in so far as they are radiating and thus accreting, are still gaining mass. Any differential growth between BHs and bulges will introduce additional scatter to the AGN $M_{\rm BH}-\sigma_*$ relation if AGN accretion and star formation are not precisely synchronized (Ho 2005; Kim et al. 2005). If we ascribe all the observed scatter to differential growth (taking the observed scatter of ~ 0.27 dex in the relation for inactive ob-

---

[1]The intrinsic scatter increases to 0.5 dex when $\sigma_{\rm H\alpha}$, rather than FWHM$_{\rm H\alpha}$ is used to estimate $M_{\rm BH}$, partly because of the difficulty of measuring the low-contrast line wings. We therefore consider only masses derived using FWHM$_{\rm H\alpha}$ in the following. We estimate that disk rotation contributes at most a small error to σ_* since we find no correlation between galaxy inclination angle and deviation from $M_{\rm BH}-\sigma_*$ (78% probability of no correlation with Kendall's τ), and typically only the inner $\sim 20\%$ of the galaxy light enters the fiber. See further arguments in Greene & Ho (2005a).

jects from Tremaine et al.), there can be no more than ~0.3 dex scatter (factor of 2) introduced by relative BH-bulge growth. This level of growth has only modest fuel requirements that are easy to sustain in nearby galaxies; a 10^6 $M_\odot$ BH requires only 0.022 $M_\odot$ yr^{-1} to double its mass in a Saltpeter time (4.5×10^7 yr).

Finally, taking our entire data set at face value, we do find evidence for a shallower slope than the inactive $M_{BH} - \sigma_*$ relation. Whether this is the result of flattening at low mass or a different slope in AGNs is difficult to determine at the present time, in the absence of more AGNs with $M_{BH} > 10^8$ $M_\odot$. In this regard, Wyithe (2005) argues that the slope for the inactive sample steepens considerably when the four smallest σ_* values are removed, independently suggesting flattening at low mass. Flattening at low mass may be a result of the changing efficiency in AGN feedback in low-mass halos. For instance, the formalism of Vittorini et al. (2005) finds that a combination of decreased optical depth (proportional to galaxy radius) and cooling times shorter than a dynamical time (small, dense halos) allows these BHs to grow to larger relative masses without feedback limitations. Alternatively, different growth modes between spheroidal and disk-dominated systems may result in a different final position on the $M_{BH} - \sigma_*$ plane. On the other hand, we cannot preclude the possibility that a change in slope in the BLR radius-luminosity relation at low luminosity is re-sponsible for the change in slope in the $M_{BH} - \sigma_*$ relation. However, we note that a radius-luminosity slope closer to the theoretically preferred value of 0.5 (e.g., Kaspi et al. 2000) would only increase the observed discrepancy in slope. Reverberation mapping of low-mass BHs would be required to address this issue.

In summary, although we have increased the population of AGNs with σ_* measurements by a factor of nearly 6, we do not yet have a large enough sample, or adequate coverage of parameter space, to uniquely identify the cause or causes responsible for the observed differences between the $M_{BH} - \sigma_*$ relation of local active and inactive galaxies. Future effort should focus on (1) further enlarging the sample of AGNs with robust σ_* measurements, (2) pushing the samples to the extremes of the mass distribution, particular above 10^8 $M_\odot$, (3) extending the luminosity coverage to include objects with a wider range in Eddington ratios, and (4) better characterizing the BLR radius-luminosity relation over a broader range of AGN properties than is currently available.

REFERENCES

Abazajian, K., et al. 2005, AJ, 129, 1755
Barth, A. J., Greene, J. E., & Ho, L. C. 2005, ApJ, 619, L151
Barth, A. J., Ho, L. C., Rutledge, R. E., & Sargent, W. L. W. 2004, ApJ, 607, 90
Blandford, R. D., & McKee, C. F. 1982, ApJ, 255, 419
Di Matteo, T., Springel, V., & Hernquist, L. 2005, Nature, 433, 604
Ferrarese, L., & Merritt, D. 2000, ApJ, 539, L9
Ferrarese, L., Pogge, R. W., Peterson, B. M., Merritt, D., Wandel, A., & Joseph, C. L. 2001, ApJ, 555, L79
Filippenko, A. V., & Ho, L. C. 2003, ApJ, 588, L13
Gebhardt, K., et al. 2000a, ApJ, 539, L13
——. 2000b, ApJ, 543, L5
Greene, J. E., & Ho, L. C. 2004, ApJ, 610, 722
——. 2005a, ApJ, 627, 721
——. 2005b, ApJ, 630, 122
——. 2005c, ApJ, in press
Hao, L., et al. 2005, AJ, 129, 1783
Ho, L. C. 1999, in Observational Evidence for the Black Holes in the Universe, ed. S. K. Chakrabarti (Dordrecht: Kluwer), 157
——. 2005, ApJ, 629, 680
Kaspi, S., Maoz, D., Netzer, H., Peterson, B. M., Vestergaard, M., & Jannuzi, B. T. 2005, ApJ, 629, 61
Kaspi, S., Smith, P. S., Netzer, H., Maoz, D., Jannuzi, B. T., & Giveon, U. 2000, ApJ, 533, 631
Kauffmann, G., & Haehnelt, M. 2000, MNRAS, 311, 576
Kim, M., Ho, L. C., & Im, M. 2005, ApJ, submitted
Murray, N., & Chiang, J. 1997, ApJ, 474, 91

Nelson, C. H., Green, R. F., Bower, G., Gebhardt, K., & Weistrop, D. 2004, ApJ, 615, 652
Netzer, H. 1990, in Active Galactic Nuclei, ed. R. D. Blandford, H. Netzer, L. Woltjer, T. Courvoisier, & M. Mayor, (Berlin: Springer), 57
Onken, C. A., Ferrarese, L., Merritt, D., Peterson, B. M., Pogge, R. W., Vestergaard, M., & Wandel, A. 2004, ApJ, 615, 645
Peng, C. Y., Impey, C. D., Ho, L. C., Barton, E. J., & Rix, H.-W. 2005, ApJ, in press (astro-ph/0509155)
Peterson, B. M., et al. 2004, ApJ, 613, 682
——. 2005, ApJ, 632, 799
Press, W. H., Teukolsky, S. A., Vetterling, W. T., & Flannery, B. P. 1992, Numerical Recipes in C (Second ed.; Cambridge: Cambridge Univ. Press), 660
Proga, D., & Kallman, T. R. 2004, ApJ, 616, 688
Proga, D., Stone, J. M., & Kallman, T. R. 2000, ApJ, 543, 686
Robertson, B., Hernquist, L., Cox, T. J., Di Matteo, T., Hopkins, P. F., Martini, P., & Springel, V. 2005, ApJ, submitted (astro-ph/0506038)
Shields, G. A., Gebhardt, K., Salviander, S., Wills, B. J., Xie, B., Brotherton, M. S., Yuan, J., & Dietrich, M. 2003, ApJ, 583, 124
Silk, J., & Rees, M. J. 1998, A&A, 331, L1
Treu, T., Malkan, M. A., & Blandford, R. D. 2004, ApJ, 615, L97
Vittorini, V., Shankar, F., & Cavaliere, A. 2005, MNRAS, 363, 1376
Walter, F., Carilli, C., Bertoldi, F., Menten, K., Cox, P., Lo, K. Y., Fan, X., & Strauss, M. A. 2004, ApJ, 615, L17
Wandel, A., Peterson, B. M., & Malkan, M. A. 1999, ApJ, 526, 579
Wyithe, S. 2005, MNRAS, submitted (astro-ph/0503435)
Yu, Q., & Lu, Y. 2004, ApJ, 610, 93
Yu, Q., & Tremaine, S. 2002, MNRAS, 335, 965